

## Chronic deep brain stimulation of the rat ventral medial prefrontal cortex disrupts hippocampal–prefrontal coherence<sup>★</sup>

Nathan Insel<sup>a,\*</sup>, Maryna Pilkiw<sup>b</sup>, José N. Nobrega<sup>a,c</sup>, William D. Hutchison<sup>e</sup>, Kaori Takehara-Nishiuchi<sup>b,d</sup>, and Clement Hamani<sup>a,e,f</sup>

<sup>a</sup>Research Imaging Centre, Centre for Addiction and Mental Health, 250 College Street, Toronto, ON M5T1R8, Canada

<sup>b</sup>Department of Psychology, University of Toronto, Toronto, ON, Canada

<sup>c</sup>Department of Psychiatry, University of Toronto, Toronto, Canada

<sup>d</sup>Department of Cell and Systems Biology, University of Toronto, Toronto, ON, Canada

<sup>e</sup>Division of Neurosurgery, Toronto Western Hospital, 399 Bathurst St., Toronto, ON M5T 2S8, Canada

<sup>f</sup>Campbell Family Mental Health Research Institute, CAMH, Canada

### Abstract

Deep brain stimulation (DBS) of the subgenual cingulate gyrus (SCG) has been used to treat patients with treatment-resistant depression. As in humans, DBS applied to the ventromedial prefrontal cortex of rats induces antidepressant-like responses. Physiological interactions between structures that play a role in depression and antidepressant treatment are still unknown. The present study examined the effect of DBS on inter-region communication by measuring the coherence of local field potentials in the rat infralimbic cortex (IL; homologue of the SCG) and one of its major afferents, the ventral hippocampus (VH). Rats received daily IL DBS treatment (100  $\mu$ A, 90  $\mu$ s, 130 Hz; 8 h/day). Recordings were conducted in unrestrained, behaving animals on the day before treatment, after 1 and 10 days of treatment, and 10 days stimulation offset. VH-IL coherence in the 2–4 Hz range was reduced in DBS-treated animals compared with shams after 10 days, but not after only 1 day of treatment. No effect of DBS was observed in the 6–10 Hz (theta) range, where coherence was generally high and could be further evoked with a loud auditory stimulus. Finally, coherence was not affected by fluoxetine (10 mg/kg), suggesting that the effects of DBS were not likely mediated by increased serotonin levels. While these data support the hypothesis that DBS disrupts communication between regions important for expectation-based control of emotion, they also suggest that lasting physiological effects require many days of treatment and, furthermore, may be specific to lower-frequency patterns, the nature and scope of which await further investigation.

<sup>★</sup>NI, MP and CH designed the experiments; NI and MP performed the experiments; NI analyzed the data; NI, JN, WDH, KT, and CH wrote the paper.

<sup>\*</sup>Corresponding author at: Research Imaging Centre, Centre for Addiction and Mental Health, 250 College Street, Toronto, ON M6T1R8, Canada. Fax: +1 416 979 4739. nathan.insel@utoronto.ca (N. Insel).

Conflicts of interest

CH is a consultant to St Jude Medical.

## Keywords

Depression; Oscillations; Synchrony; Delta; Functional connectivity

---

## Introduction

Deep brain stimulation (DBS) of the subgenual cingulate gyrus (SCG) can be effective at alleviating depression symptoms in patients who are otherwise treatment-resistant (Mayberg et al., 2005; Lozano et al., 2008). Previous experiments from our lab have found that DBS applied to the rodent ventral medial prefrontal cortex (vmPFC) can also induce antidepressant-like effects (Hamani et al., 2010, 2012, 2014). This treatment model has provided a tool to directly probe how the nervous system is affected by stimulation and how physiological consequences are linked to depression. For example, recent work found that patterns of immediate early gene (IEG) expression across regions become less correlated between animals who have received vmPFC stimulation compared with correlations between non-stimulated animals (Hamani et al., 2014; Wheeler et al., 2013). This observation can be considered alongside demonstrations that brains of depressed patients exhibit abnormally high activity correlations (“functional connectivity”) between the SCG and connected regions (Greicius et al., 2007; Berman et al., 2011; Zeng et al., 2012; Sambataro et al., 2013; Davey et al., 2012), raising the question of whether DBS may disrupt communication between brain networks that become pathologically hyperactive in depression. Precisely how DBS affects neural signaling between brain regions, and which physiological processes might underlie depression-related changes in inter-region activity correlations, remains unclear.

In the present set of experiments we test the hypothesis that chronic stimulation of the vmPFC disrupts communication with a major afferent, the ventral hippocampus (VH). We specifically target the infralimbic cortex (IL), because this region in particular may be part of the rodent homologue of the SCG, and because it shows the highest density of projections from VH (Swanson, 1981). We record local field potentials (LFPs) from both regions in freely-moving rats before as well as after multiple days of high-frequency electrical stimulation.

## Methods

### Experimental subjects, surgeries, and histology

All procedures were approved by the University of Toronto Animal Care Committee and the Animal Care Committee of the Centre for Addiction and Mental Health. Experimental subjects were 15 male, Sprague–Dawley rats between 2 1/2 to 4 months old (Charles River). Following habituation to our animal facility, the animals were randomly assigned to those receiving DBS (n = 8) or sham stimulation (n = 7; electrodes implanted with no stimulation being delivered).

Surgeries were performed under isoflurane anesthesia. In each rat, monopolar stimulating electrodes (250  $\mu$ m diameter with approximately 100  $\mu$ m of insulation removed at tips) were

placed bilaterally into the IL (3.0 mm anterior and 0.8 mm to the left and right of bregma lowered 4.4 mm ventral from the brain surface). One stainless steel (76  $\mu\text{m}$  diameter bare, 140  $\mu\text{m}$  coated) electrode was twisted around the right-side stimulating electrode to record local field potentials (LFPs), with tips of the two electrodes estimated to be 50 to 200  $\mu\text{m}$  from one-another. Using different electrodes for stimulation and recording ensured that observed physiological changes could not be explained by stimulation effects on the tissue immediately adjacent to the electrode tip. A second LFP recording electrode was placed in the CA1 subfield of the ventral hippocampus (6 mm posterior and 5.7 mm to the right of bregma, lowered 6.2 mm from the brain surface). Approximate target locations are illustrated in Fig. 1A. A third stainless steel electrode was implanted into the cerebellum to be used as reference. A ground screw placed above the parietal cortex was wired to the ground of the recording equipment and used as an alternative reference channel. Rats were given at least two days of recovery from implantation surgery before recordings and treatment began.

Following the experiment, the rats were administered an overdose of sodium pentobarbital and perfused with 4% paraformaldehyde. Electrode location was confirmed in Nissl-stained sections (Fig. 1B).

### Schedule of recording sessions and treatments

Fig. 1C shows the timeline of the experiments. Each recording session took place in a 50  $\times$  50 cm square box where rats were allowed to move freely and involved three recording epochs. The first fifteen minutes of the session together constituted the “spontaneous behavior” epoch. This was followed by the “auditory stimulation” epoch, during which a brief auditory tone (100 ms, 2.5 kHz, 95 DB) was presented from speakers placed 50 cm above the rat. The tone was repeated 80 times over 33 min, each pulse presented between 20–30 s following the previous. The purpose of the auditory stimulation was to evoke attentional responses that provided a temporal reference for the analysis of neural activity. Following auditory stimulation, recording sessions continued for another 45 min, the “rest” epoch, to allow further investigation of physiological patterns across animals' activity states.

Data were collected in 5 or 6 recording sessions for each rat. The first recording session took place one day prior to the first day of DBS or sham treatment (Day 0). Other recording sessions took place in the evening or night (near the transition of rats' dark-to-light cycles) after 1 day of treatment, after 10 days of treatment, and 10 days following the termination of treatment (Day Post-10). An additional recording session took place (Day Post-1 or Post-11) while rats were injected with the selective serotonin reuptake inhibitor (SSRI) fluoxetine (10 mg/kg). As a control for the effects of injections, a subset of animals (4 DBS, 3 sham) was also recorded from after a single saline injection (Day Post-1). During injection days, protocols included pre- (15 min) and post-injection (30 min) baseline recording periods. These epochs were followed by a 33 min auditory stimulation epoch and a shortened (approximately 20 min) rest epoch.

DBS treatments consisted of 8 continuous hours of unipolar stimulation (90  $\mu\text{s}$  pulses of 100  $\mu\text{A}$  at 130 Hz) delivered bilaterally to the IL. Treatments were administered in each rat's home cage by a handheld medical stimulator (St. Jude Medical model 6510; Plano, Texas),

interfaced by a headcap and cable (Plastics One, Roanoke, VA) and commutator to ensure freedom of movement. Rats receiving sham stimulation were connected on the same days that DBS rats were connected but stimulators were not turned on.

### Data collection

Behavioral and neural data were acquired during each recording session. Movements were monitored by an overhead camera (14 Hz frame rate) tracking red LEDs attached to the headcap. Movement data was synchronized with neural data using a custom-built program in Python (<https://www.python.org/>) implementing the OpenCV library (<http://opencv.org/>). Position information was computed from video using a custom-written program in MATLAB (MathWorks; Natick, MA). Neural data was collected using a Tucker Davis Technologies (Alachua, FL) RZ5D system and consisted of LFPs sampled at 2034 Hz and filtered between 0.1 and 400 Hz, collected from the right infralimbic cortex and the right ventral hippocampus. All were referenced against the cerebellar electrode. The cerebellar reference electrode was recorded against the ground screw to allow for re-referencing.

### Data analysis

**Coherence during spontaneous behavior**—All analyses were implemented in MATLAB. Coherence measures relied on a multitaper technique provided within the Chronux toolbox (<http://www.chronux.org/>). LFP signals during the first 15 min of recording (the spontaneous behavior epoch) were segmented into non-overlapping, 10 s windows. Three to five tapers were applied to each window and a Fast-Fourier Transform was used to compute spectra of LFPs recorded in each individual regions and the cross spectra between regions. Coherence was defined as the square of the cross-spectra divided by the product of the individual spectra (i.e., magnitude squared coherence). These scores were then averaged across windows. The frequency resolution for the chosen sampling rate and window length was 0.06 Hz.

**Signal amplitude during spontaneous behavior**—LFP signal amplitude can vary according to non-physiological factors such as electrode impedance and precise position. To standardize measurements of LFP spectra across animals we used the relative amplitude of one frequency component compared with another. As described in the Results, theta (6 to 10 Hz) coherence was not found to significantly change with DBS treatments; we therefore used the ratio of 2–4 Hz to theta amplitude as our dependent variable.

**Movement and coherence**—Instantaneous velocity was computed for each 14 Hz (about 71 ms) sampled video interval from the position information. To reduce the impact of jitter, video data were first smoothed by convolving with a 10-sample (roughly 700 ms) hamming window (analyses were additionally run on non-smoothed data for confirmation). Total movement in a session was then calculated as the cumulative sum of instantaneous velocity divided by the video sampling rate. Orienting responses to the auditory stimulus were quantified by averaging the stimulus-aligned instantaneous velocity traces. The relationship between LFP coherence and movement was evaluated by binning instantaneous velocity vectors into 714 ms intervals (i.e., converting 14 Hz signals to 1.4 Hz). From these, 80 bins were selected at random that fell within 1 cm/s intervals, up to 20 cm/s. The 80 bins for a

given velocity window were treated as “trials,” over which signal amplitude and coherence were computed at both 2–4 Hz and 6–10 Hz frequency bands.

**Stimulus-related coherence and amplitude**—Instantaneous measures of amplitude and coherence were computed so that stimulus-related changes could be evaluated. Amplitude of 2–4 Hz and 6–10 Hz LFP patterns was computed by first filtering the signals at the respective frequency bands with a 3rd order, Chebyshev Type I filter and then taking the absolute value of the Hilbert transformation. For improved temporal resolution, phase correlations were measured not with magnitude squared coherence but by using a phase synchronization method. To compute phase differences between the two regions, signals were 1) filtered as just described, 2) transformed using the Hilbert transform, 3) converted to phase values by taking the arctangent of real and imaginary components, 4) subtracted one from the other using circular subtraction, and 5) the result was averaged over window lengths of 500 ms (2–4 Hz) or 200 ms (6–10 Hz), stepped at 250 and 100 ms respectively.

**Significance testing**—Significance was assessed by comparing scores between animal groups, as described on a case-by-case basis in the Results. In most cases, scores across animals were assumed to vary according to a Gaussian distribution, and we therefore often applied *t*-tests and ANOVAs.

## Results

### Effects of DBS on VH-IL coherence during spontaneous behavior

Coherence between the ventral hippocampus and the infralimbic cortex was significantly reduced in low frequency bands following 10 days of DBS treatment as compared against sham controls (Fig. 2A). To control for behavioral state, these initial analyses considered only the first 15 min after rats were placed in the environment before auditory cues were presented (i.e., the spontaneous behavior epoch). The coherence difference during this time exceeded 99% confidence limits (estimated using independent sample *t*-tests) for a continuous frequency range between 1.3 to 4.3 Hz, but was particularly robust between 2 to 4 Hz (Fig. 2B; independent sample *t*-test comparing 2–4 Hz coherence in sham and DBS:  $p = 3.6 \times 10^{-3}$ ; paired *t*-test on DBS group day 10 vs. day 0:  $p = 0.022$ ; 2-way repeated measures ANOVA test for interaction between treatment and stimulation day:  $F(3,56) = 3.61$ ,  $p = 0.023$ ). Although some frequency bins within the 10–15 Hz range met the 99% criteria, there were notably no differences in the 6–10 Hz (theta) band, where coherence between the two regions was highest, or in frequencies above 15 Hz (computed for all frequency bins below 100 Hz).

To gain more information on whether DBS influenced the VH-IL connection specifically, or whether it caused more general changes in 2–4 Hz brain activity, we examined DBS effects on LFPs separately in each region. Low frequency (2–4 Hz) amplitude was measured relative to theta amplitude to control for electrode impedance and other non-physiological variables (see Methods). In the IL, the ratio of 2–4 Hz to theta amplitude did not differ between DBS and sham animals either before treatment (independent sample *t*-test:  $p = 0.84$ ) or after ten days of treatment ( $p = 0.94$ ; Figs. 2C & D). In the VH, no difference was observed before treatment ( $p = 0.21$ ) but there appeared to be reduced, relative 2–4 Hz

amplitude in the DBS animals over days ( $t$ -test between groups at 10 days:  $p = 0.074$ , significant using a one-tailed test; repeated measures ANOVA test for interaction between treatment group and relative 2–4 Hz amplitude across days:  $F(3,56) = 3.89$ ,  $p = 0.017$ ; Figs. 2E & F). Additionally, the relative amplitude of hippocampal 2–4 Hz activity was directly correlated with coherence between the regions ( $r = 0.57$ ,  $p = 0.028$ ). The data were thus consistent with a general or indirect effect of DBS on brain activity in the 2–4 Hz range.

We next investigated the relationship between coherence changes and behavior. If VH-IL coherence is correlated with behavior on a moment-by-moment basis, then it raises the question of whether the physiological change is an epiphenomenon of altered behavior. Instantaneous velocity was computed for each ~70 ms interval (14 Hz—the temporal resolution of the camera) of each recording session. No differences were observed in the average, cumulative movement of DBS and sham-treated animals after ten days of stimulation (Fig. 3A; independent sample  $t$ -test at 15 min:  $p = 0.17$ , at 100 min:  $p = 0.36$ ). Nor were movement responses found to differ between the two groups when rats were presented with a loud auditory stimulus (Fig. 3B; two-sample  $t$ -test of cue-locked averages of instantaneous velocity, at peak response:  $p = 0.82$ ). Moreover, VH-IL coherence in the 2–4 Hz range did not vary with how fast the rat was moving at a given time (Fig. 3C, top-left panels). This was evaluated statistically by applying a regression model that included variables for velocity, day, treatment group, and an interaction variable of treatment group-by-day. Only coefficients for treatment group and the group-by-day interaction variable statistically differed from zero (based on both 95 and 99% confidence limits). In contrast, coherence in the theta band changed across days, but no interaction was observed between treatment group and days (again based on both 95% and 99% confidence limits). Although coherence did not vary with velocity, the amplitude of both 2–4 Hz and theta activity did. This was true in both the VH (Fig. 3C, middle panels) and the IL (lower panels).

### Effects of DBS on VH-IL coherence following stimulus presentation

To gain more insight into the underlying cognitive or computational processes that 2–4 Hz coherence between VH and IL may relate to, we examined how coherence was affected by the presentation of a loud auditory cue (during which rats were arguably in an alert, attentive, and potentially anxious state). Presentation of an auditory stimulus evoked several characteristic LFP wave patterns in both the IL and VH (Figs. 4A & B). The relative contribution of 2–4 Hz and theta oscillations to these “event related potentials,” were assessed by comparing the amplitudes of the two frequency bands immediately before versus after cue presentation (i.e., based on cue-locked averages of the filtered and rectified signals). Activity in the theta frequency was significantly increased in both regions during the first one-second after stimulus-presentation relative to the preceding second (Figs. 4C & D;  $n = 15$  rats,  $t$ -test comparing z-score normalized averages on the pre-treatment, Day 0 session; IL:  $p = 4.1 \times 10^{-4}$ ; VH:  $p = 0.03$ ). In contrast, taking into account a slightly longer time period, slower, 2–4 Hz activity patterns decreased in both regions following presentation of sounds (Figs. 4E & F; comparing 2 s after vs. 2 s before, IL:  $p = 0.0065$ , VC:  $p = 0.012$ ). Stimulus-evoked effects on coherence between regions paralleled changes in power, with increases observed in theta coherence (Fig. 4G; measured continuously using a phase synchrony method, as described in Methods;  $p = 0.040$ ), and decreases in the 2–4 Hz

band (Fig. 4H;  $p = 0.023$ ). Note that while significant increases in theta synchrony following stimulus presentation were also observed on all subsequent recording sessions, the decreases in 2–4 Hz synchrony were only observed on Day 0. Altogether, however, there was no evidence that stimulus-evoked changes were influenced by DBS treatment (Figs. 4I & J).

### Effects of fluoxetine on VH-IL coherence

The most common pharmacological treatment for depression is selective serotonin reuptake inhibitors (SSRIs), which can acutely increase synaptic serotonin levels throughout the brain, including within the medial prefrontal cortex (Beyer and Cremers, 2008) and the hippocampus (Sabol et al., 1992). To determine whether serotonin increases influence VH-IL coherence, we recorded from the same rats that had received DBS or sham treatments after they had been injected with the SSRI fluoxetine ( $n = 15$ ) and, during a separate session, injected with saline ( $n = 7$ ). Comparisons between fluoxetine and saline values failed significance testing for all individual frequency bins (independent sample  $t$ -tests,  $\alpha = 0.05$ ; Fig. 5A) and for  $\delta$ averaged values within the 2–4 Hz band ( $p = 0.66$ ). There were also no interactions between prior DBS treatment and fluoxetine injection on coherence spectra (Fig. 5B). Fluoxetine did not decrease the amplitude of 2–4 Hz activity, relative to theta amplitude, in either the IL (Fig. 5C) or VH (Fig. 5D). Finally, fluoxetine did not appear to influence the degree to which IL-VH phase synchronization was affected by presentation of the auditory stimulus (Figs. 5E & F).

### Discussion

The present experiments were designed to investigate the hypothesis that DBS treatments of depression reduce communication between specific neural pathways thought to be overactive in depressed patients. We specifically chose to examine the IL because of convergent evidence that the human homologue, the SCG, behaves abnormally in depression (Mayberg et al., 1999; Kennedy et al., 2001; Drevets et al., 2002), and chose the VH because it provides a major, unreciprocated projection to the IL (Swanson, 1981; Jay et al., 1989; Jay and Witter, 1991; Hoover and Vertes, 2007; Jones and Witter, 2007). To make inferences about communication between these regions we measured coherence of the respective local field potentials. The data confirmed that VH and IL activity become less correlated following DBS treatments, but the reduction is primarily restricted to the 2–4 Hz frequency band. Changes were not evident after a single day of treatment, but could be observed after ten days. They also were strongest when rats were awake and spontaneously exploring the environment, although they did not vary with movement speed on a moment-by-moment basis, suggesting that the communication change was relevant for online processing but was not directly driven by, or driving, sensorimotor activity.

This experiment had several limitations. Most notable was the inability to record neural signals during the stimulation itself. However, although clinical studies report immediate effects of SCG DBS, they also report progressive improvements in depressive symptoms over the course of weeks and months, which can be subsequently maintained for several weeks following cessation of stimulation (e.g., Mayberg et al., 2005). It is therefore interesting that the physiological effects observed in the present study were observed only at

the longer, 10 day time point, and not after only one day, suggesting that only long-term treatment was sufficient to induce those plasticity processes supporting the coherence changes.

What, then, might be the specific plasticity processes that result in altered coherence after ten days of DBS treatment? This question speaks to a second limitation of the experiment: by targeting the VH-IL circuit specifically, it is difficult to know whether the coherence changes were unique to this circuit or reflected more global changes in brain activity. Synapses connecting VH to IL can be modified by experience (reviewed by Laroche et al., 2000), and a straightforward explanation of DBS-mediated coherence reductions is reduced synaptic strength resulting from chronic stimulation of the post-synaptic area (the IL) in the absence of chronic presynaptic (VH) neuron activity. However, two other observations seem inconsistent with this view. First, coherence changes were not observed in the theta frequency band, within which these regions are known to interact; it is not clear why generalized decreases in synaptic depression might only affect low-frequency activity correlations. Second, decreased 2–4 Hz coherence was correlated with, and therefore potentially a result of, decreased 2–4 Hz activity patterns locally within the VH (notably, not in the IL) as measured by amplitude relative to the 6–10 Hz theta frequency. These observations can be considered alongside other data on hippocampal–prefrontal coherence patterns to build a case for a more generalized effect of IL stimulation, one that may also include the catecholamine system.

VH-IL coherence in both treatment groups was strongest within the 6 to 10 Hz theta frequency band. These data are consistent with previous examinations of communication between the medial prefrontal cortex and hippocampus of rodents (Siapas et al., 2005; Jones and Wilson, 2005a, 2005b; Hyman et al., 2005, 2010; Sirota et al., 2008; Hartwich et al., 2009; Young and McNaughton, 2009; Adhikari et al., 2010; Benchenane et al., 2010; also reviewed by Colgin, 2011). Most research in this area has looked at neural activity correlations between the dorsal hippocampus and the prelimbic cortex, located just dorsal to the IL, and patterns have been linked to cognitive variables such as working memory (Jones and Wilson, 2005b; Hyman et al., 2005) and expectation-based decision-making (Benchenane et al., 2010). Meanwhile, coherence between the VH and the prelimbic cortex has been linked to anxiety (Adhikari et al., 2010). This is not inconsistent with the present observation that theta amplitude and coherence increases following presentation of loud auditory cues.

Importantly, we found that DBS did not affect theta coherence, but rather coherence in the 2 to 4 Hz band. In contrast with theta, correlated activity patterns in the 2 to 4 Hz range during waking have been treated with less depth and may in some cases have been overlooked. Spectral power in this range is normally referred to as either “delta” or “slow-theta.” Although delta is defined as 1–4 Hz activity, it is typically used to refer to a specific phenomenon taking place during non-REM sleep, characterized by transitions between low-activity (“DOWN”) to high-activity (“UP”) network states, and mediated by interactions between cortex and thalamus (Steriade et al., 1993). In the present study, coherence between 2 and 4 Hz was not found to change between movement and non-movement. Theta oscillations, meanwhile, can be as slow as 4 Hz, particularly in motionless animals (referred



to by Vanderwolf and colleagues as Type II theta; Kramis et al., 1975). In the present experiment, the strong theta oscillation at 6 to 10 Hz exhibited very different relationships to movement speed and tone presentation compared with 2 to 4 Hz activity. Taken together, it is possible that 2–4 Hz coherence shares neither the same mechanisms nor the same functions as theta or sleep-related delta oscillations. What those mechanisms and functions are, however, remains unclear. The most thorough examination of this frequency band in the behaving rodent may be that of Fujisawa and Buzsáki (2011), who found that coherence between 2 and 5 Hz increased between the ventral tegmental area (VTA) and prelimbic cortex during an odor-to-place matching task, and that this oscillation was phase-coupled with theta in the dorsal hippocampus. This report extended previous observations that VTA neurons often fire action potentials at regular intervals of 4 Hz (Hyland et al., 2002; Paladini and Tepper, 1999; Bayer et al., 2007; Dzirasa et al., 2010; Kobayashi and Schultz, 2008). Hippocampal–prefrontal coherence in the 4 Hz band can also increase when dopamine is injection directly into the prefrontal cortex (Benchenane et al., 2010). The emphasis on dopamine in these examples may be misleading, in that the dopamine system has received disproportionate experimental attention, and might be only one of many systems participating in neural changes at 2 to 4 Hz. In the present experiment, coherence in this frequency domain was not found to be influenced by fluoxetine injection, and therefore is unlikely to be related to serotonin concentrations.

Aside from the question about the underlying mechanisms of 2–4 Hz coherence changes is the question of how these observations can be used to inform clinical diagnosis or treatment. Previous work using electroencephalograms (EEGs) to examine inter-region coherence in depressed versus control patients have yielded complex results, with differences found in the proximity of electrode pairs, their hemisphere, and frequency bands (Fingelkurts et al., 2007; Leuchter et al., 2012). The effects on EEG of treatment with SCG DBS are also complex, although generally appear to make depressed brains appear more similar to non-depressed controls (Broadway et al., 2012; Quraan et al., 2014). The source of complexity in these results is unclear, and might reflect effects from any number of interacting variables common to human depression or its treatment-related relief. By identifying a particular frequency band affected by frontal DBS within a particular neural circuit, and controlling for many potential confounds in clinical populations by using an animal model that has not been otherwise manipulated, the present results may be tapping into a primary consequence of stimulation treatments. Future clinical examinations may therefore find value in focusing on 2–4 Hz activity in the hippocampus (such as by using LORETA or other advanced localization techniques), or other affected regions, as a marker for the primary effects of SCG DBS on the brain.

In summary, the present data provide evidence consistent with the theory that chronic DBS treatments disrupt communication between regions of the limbic system, namely, the VH and IL. They are consistent with the hypothesis that depression involves hyperactive communication between emotion-processing regions of the brain that include the IL, while also raising a number of questions about the source, scope, and function of brain oscillations in the 2 to 4 Hz range.

## Acknowledgments

This work was supported by Canadian Institutes of Health Research Grant 110970.

## Abbreviations

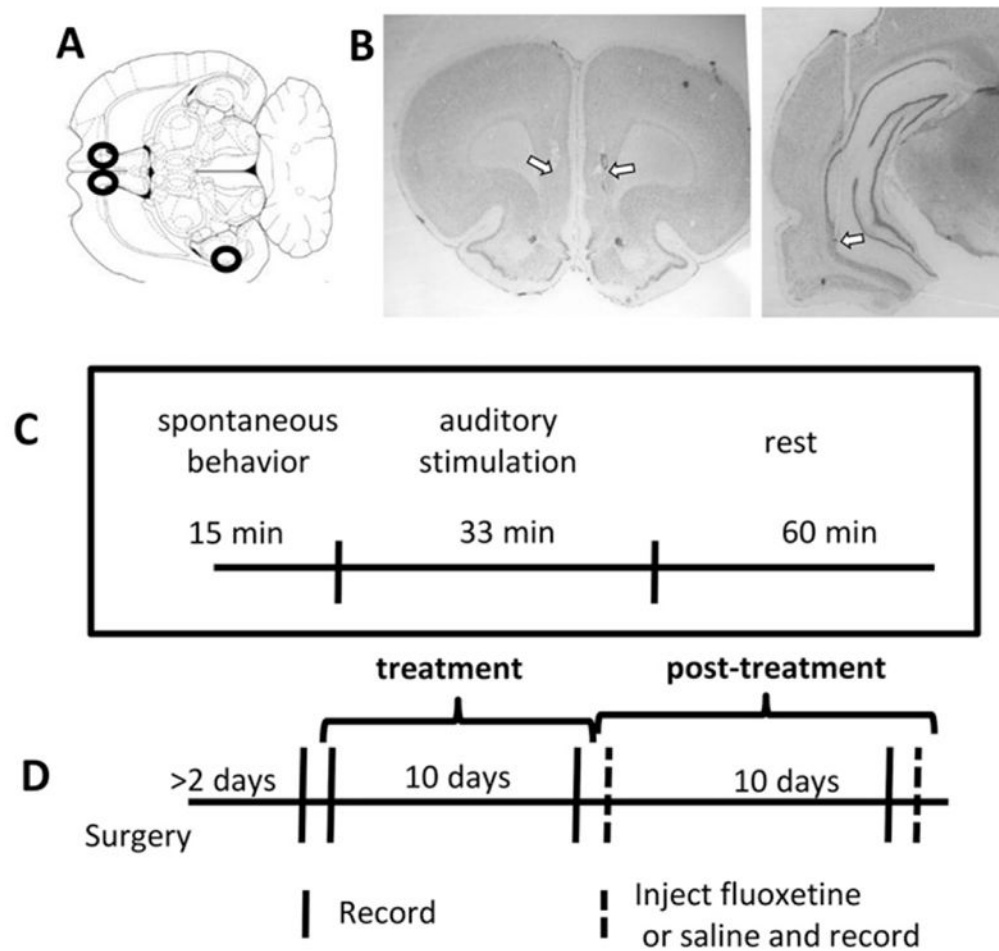
<b>SCG</b>	subgenualcingulategyrus
<b>IL</b>	infralimbiccortex
<b>VH</b>	ventralhippo-campus
<b>LFP</b>	local field potential

## References

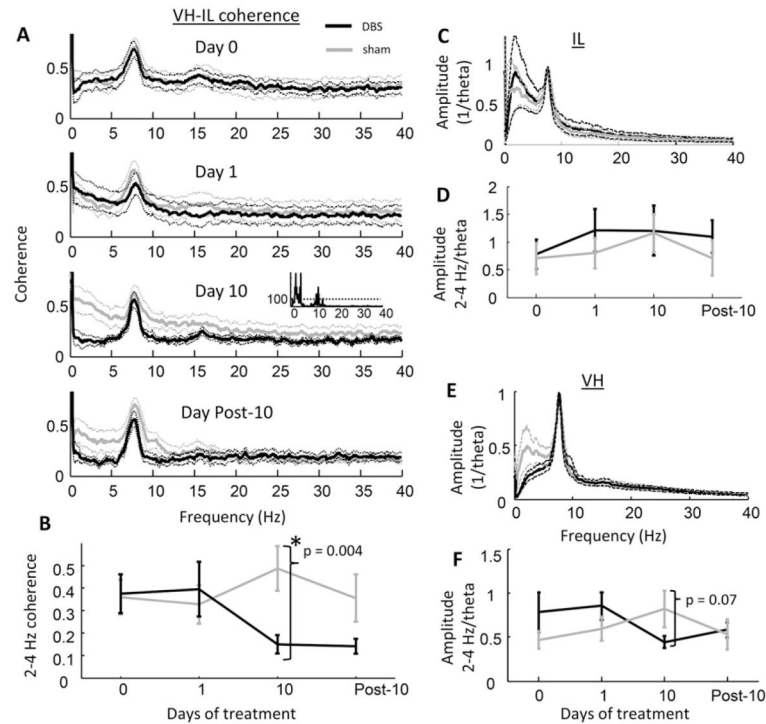
- Adhikari A, Topiwala MA, Gordon JA. Synchronized activity between the ventral hippocampus and the medial prefrontal cortex during anxiety. *Neuron*. 2010; 65:257–269. <http://dx.doi.org/10.1016/j.neuron.2009.12.002>. [PubMed: 20152131]
- Bayer HM, Lau B, Glimcher PW. Statistics of midbrain dopamine neuron spike trains in the awake primate. *J Neurophysiol*. 2007; 98:1428–1439. <http://dx.doi.org/10.1152/jn.01140.2006>. [PubMed: 17615124]
- Benchenane K, Peyrache A, Khamassi M, Tierney PL, Gioanni Y, Battaglia FP, Wiener SI. Coherent theta oscillations and reorganization of spike timing in the hippocampal–prefrontal network upon learning. *Neuron*. 2010; 66:921–936. <http://dx.doi.org/10.1016/j.neuron.2010.05.013>. [PubMed: 20620877]
- Berman MG, Peltier S, Nee DE, Kross E, Deldin PJ, Jonides J. Depression, rumination and the default network. *Soc Cogn Affect Neurosci*. 2011; 6:548–555. <http://dx.doi.org/10.1093/scan/nsq080>. [PubMed: 20855296]
- Beyer CE, Cremers TIFH. Do selective serotonin reuptake inhibitors acutely increase frontal cortex levels of serotonin? *Eur J Pharmacol*. 2008; 580:350–354. <http://dx.doi.org/10.1016/j.ejphar.2007.11.028>. [PubMed: 18177637]
- Broadway JM, Holtzheimer PE, Hilimire MR, Parks NA, Devylder JE, Mayberg HS, Corballis PM. Frontal theta cordance predicts 6-month antidepressant response to subcallosal cingulate deep brain stimulation for treatment-resistant depression: a pilot study. *Neuropsychopharmacology*. 2012; 37:1764–1772. <http://dx.doi.org/10.1038/npp.2012.23>. [PubMed: 22414813]
- Colgin LL. Oscillations and hippocampal–prefrontal synchrony. *Curr Opin Neurobiol*. 2011; 21:467–474. <http://dx.doi.org/10.1016/j.conb.2011.04.006>. [PubMed: 21571522]
- Davey CG, Yücel M, Allen NB, Harrison BJ. Task-related deactivation and functional connectivity of the subgenual cingulate cortex in major depressive disorder. *Front Psychiatry*. 2012; 3:14. <http://dx.doi.org/10.3389/fpsy.2012.00014>. [PubMed: 22403553]
- Drevets WC, Bogers W, Raichle ME. Functional anatomical correlates of antidepressant drug treatment assessed using PET measures of regional glucose metabolism. *Eur Neuropsychopharmacol*. 2002; 12:527–544. [PubMed: 12468016]
- Dzirasa K, Coque L, Sidor MM, Kumar S, Dancy EA, Takahashi JS, McClung CA, Nicolelis MAL. Lithium ameliorates nucleus accumbens phase-signaling dysfunction in a genetic mouse model of mania. *J Neurosci*. 2010; 30:16314–16323. <http://dx.doi.org/10.1523/JNEUROSCI.4289-10.2010>. [PubMed: 21123577]
- Fingelkurts AA, Fingelkurts AA, Rytälä H, Suominen K, Isometsä E, Kähkönen S. Impaired functional connectivity at EEG alpha and theta frequency bands in major depression. *Hum Brain Mapp*. 2007; 28:247–261. <http://dx.doi.org/10.1002/hbm.20275>. [PubMed: 16779797]
- Fujisawa S, Buzsáki G. A 4 Hz oscillation adaptively synchronizes prefrontal, VTA, and hippocampal activities. *Neuron*. 2011; 72:153–165. <http://dx.doi.org/10.1016/j.neuron.2011.08.018>. [PubMed: 21982376]

- Greicius MD, Flores BH, Menon V, Glover GH, Solvason HB, Kenna H, Reiss AL, Schatzberg AF. Resting-state functional connectivity in major depression: abnormally increased contributions from subgenual cingulate cortex and thalamus. *Biol Psychiatry*. 2007; 62:429–437. <http://dx.doi.org/10.1016/j.biopsych.2006.09.020>. [PubMed: 17210143]
- Hamani C, Diwan M, Macedo CE, Brandão ML, Shumake J, Gonzalez-Lima F, Raymond R, Lozano AM, Fletcher PJ, Nobrega JN. Antidepressant-like effects of medial prefrontal cortex deep brain stimulation in rats. *Biol Psychiatry*. 2010; 67:117–124. <http://dx.doi.org/10.1016/j.biopsych.2009.08.025>. [PubMed: 19819426]
- Hamani C, Machado DC, Hipólido DC, Dubiela FP, Suchecki D, Macedo CE, Tescarollo F, Martins U, Covolan L, Nobrega JN. Deep brain stimulation reverses anhedonic-like behavior in a chronic model of depression: role of serotonin and brain derived neurotrophic factor. *Biol Psychiatry*. 2012; 71:30–35. <http://dx.doi.org/10.1016/j.biopsych.2011.08.025>. [PubMed: 22000731]
- Hamani C, Amorim BO, Wheeler AL, Diwan M, Driesslein K, Covolan L, Butson CR, Nobrega JN. Deep brain stimulation in rats: different targets induce similar antidepressant-like effects but influence different circuits. *Neurobiol Dis*. 2014; 71:205–214. <http://dx.doi.org/10.1016/j.nbd.2014.08.007>. [PubMed: 25131446]
- Hartwich K, Pollak T, Klausberger T. Distinct firing patterns of identified basket and dendrite-targeting interneurons in the prefrontal cortex during hippocampal theta and local spindle oscillations. *J Neurosci*. 2009; 29:9563–9574. <http://dx.doi.org/10.1523/JNEUROSCI.1397-09.2009>. [PubMed: 19641119]
- Hoover WB, Vertes RP. Anatomical analysis of afferent projections to the medial prefrontal cortex in the rat. *Brain Struct Funct*. 2007; 212:149–179. <http://dx.doi.org/10.1007/s00429-007-0150-4>. [PubMed: 17717690]
- Hyland BI, Reynolds JNJ, Hay J, Perk CG, Miller R. Firing modes of midbrain dopamine cells in the freely moving rat. *Neuroscience*. 2002; 114:475–492. [PubMed: 12204216]
- Hyman JM, Zilli EA, Paley AM, Hasselmo ME. Medial prefrontal cortex cells show dynamic modulation with the hippocampal theta rhythm dependent on behavior. *Hippocampus*. 2005; 15:739–749. <http://dx.doi.org/10.1002/hipo.20106>. [PubMed: 16015622]
- Hyman JM, Zilli EA, Paley AM, Hasselmo ME. Working memory performance correlates with prefrontal–hippocampal theta interactions but not with prefrontal neuron firing rates. *Front Integr Neurosci*. 2010; 4:2. <http://dx.doi.org/10.3389/neuro.07.002.2010>. [PubMed: 20431726]
- Jay TM, Witter MP. Distribution of hippocampal CA1 and subicular efferents in the prefrontal cortex of the rat studied by means of anterograde transport of *Phaseolus vulgaris*-leucoagglutinin. *J Comp Neurol*. 1991; 313:574–586. <http://dx.doi.org/10.1002/cne.903130404>. [PubMed: 1783682]
- Jay TM, Glowinski J, Thierry AM. Selectivity of the hippocampal projection to the prelimbic area of the prefrontal cortex in the rat. *Brain Res*. 1989; 505:337–340. [PubMed: 2598054]
- Jones MW, Wilson MA. Phase precession of medial prefrontal cortical activity relative to the hippocampal theta rhythm. *Hippocampus*. 2005a; 15:867–873. <http://dx.doi.org/10.1002/hipo.20119>. [PubMed: 16149084]
- Jones MW, Wilson MA. Theta rhythms coordinate hippocampal–prefrontal interactions in a spatial memory task. *PLoS Biol*. 2005b; 3:e402. <http://dx.doi.org/10.1371/journal.pbio.0030402>. [PubMed: 16279838]
- Jones BF, Witter MP. Cingulate cortex projections to the parahippocampal region and hippocampal formation in the rat. *Hippocampus*. 2007; 17:957–976. <http://dx.doi.org/10.1002/hipo.20330>. [PubMed: 17598159]
- Kennedy SH, Evans KR, Krüger S, Mayberg HS, Meyer JH, McCann S, Arifuzzman AI, Houle S, Vaccarino FJ. Changes in regional brain glucose metabolism measured with positron emission tomography after paroxetine treatment of major depression. *Am J Psychiatry*. 2001; 158:899–905. [PubMed: 11384897]
- Kobayashi S, Schultz W. Influence of reward delays on responses of dopamine neurons. *J Neurosci*. 2008; 28:7837–7846. <http://dx.doi.org/10.1523/JNEUROSCI.1600-08.2008>. [PubMed: 18667616]
- Kramis R, Vanderwolf CH, Bland BH. Two types of hippocampal rhythmical slow activity in both the rabbit and the rat: relations to behavior and effects of atropine, diethyl ether, urethane, and pentobarbital. *Exp Neurol*. 1975; 49:58–85. [PubMed: 1183532]

- Laroche S, Davis S, Jay TM. Plasticity at hippocampal to prefrontal cortex synapses: dual roles in working memory and consolidation. *Hippocampus*. 2000; 10:438–446. [http://dx.doi.org/10.1002/1098-1063\(2000\)10:4<438::AID-HIPO10>3.0.CO;2-3](http://dx.doi.org/10.1002/1098-1063(2000)10:4<438::AID-HIPO10>3.0.CO;2-3). [PubMed: 10985283]
- Leuchter AF, Cook IA, Hunter AM, Cai C, Horvath S. Resting-state quantitative electroencephalography reveals increased neurophysiologic connectivity in depression. *PLoS One*. 2012; 7:e32508. <http://dx.doi.org/10.1371/journal.pone.0032508>. [PubMed: 22384265]
- Lozano AM, Mayberg HS, Giacobbe P, Hamani C, Craddock RC, Kennedy SH. Subcallosal cingulate gyrus deep brain stimulation for treatment-resistant depression. *Biol Psychiatry*. 2008; 64:461–467. <http://dx.doi.org/10.1016/j.biopsych.2008.05.034>. [PubMed: 18639234]
- Mayberg HS, Liotti M, Brannan SK, McGinnis S, Mahurin RK, Jerabek PA, Silva JA, Tekell JL, Martin CC, Lancaster JL, Fox PT. Reciprocal limbic-cortical function and negative mood: converging PET findings in depression and normal sadness. *Am J Psychiatry*. 1999; 156:675–682. <http://dx.doi.org/10.1176/ajp.156.5.675>. [PubMed: 10327898]
- Mayberg HS, Lozano AM, Voon V, McNeely HE, Seminowicz D, Hamani C, Schwab JM, Kennedy SH. Deep brain stimulation for treatment-resistant depression. *Neuron*. 2005; 45:651–660. <http://dx.doi.org/10.1016/j.neuron.2005.02.014>. [PubMed: 15748841]
- Paladini CA, Tepper JM. GABA(A) and GABA(B) antagonists differentially affect the firing pattern of substantia nigra dopaminergic neurons in vivo. *Synapse*. 1999; 32:165–176. [http://dx.doi.org/10.1002/\(SICI\)1098-2396\(19990601\)32:3<165::AID-SYN3>3.0.CO;2-N](http://dx.doi.org/10.1002/(SICI)1098-2396(19990601)32:3<165::AID-SYN3>3.0.CO;2-N). [PubMed: 10340627]
- Paxinos, G., Watson, C. *The Rat Brain in Stereotaxic Coordinates*. 4. Academic Press; San Diego: 1998.
- Quraan MA, Protzner AB, Daskalakis ZJ, Giacobbe P, Tang CW, Kennedy SH, Lozano AM, McAndrews MP. EEG power asymmetry and functional connectivity as a marker of treatment effectiveness in DBS surgery for depression. *Neuropsychopharmacology*. 2014; 39:1270–1281. <http://dx.doi.org/10.1038/npp.2013.330>. [PubMed: 24285211]
- Sabol KE, Richards JB, Seiden LS. Fluoxetine attenuates the DL-fenfluramine-induced increase in extracellular serotonin as measured by in vivo dialysis. *Brain Res*. 1992; 585:421–424. [PubMed: 1511330]
- Sambataro, F., Wolf, ND., Pennuto, M., Vasic, N., Wolf, RC. Revisiting default mode network function in major depression: evidence for disrupted subsystem connectivity; *Psychol Med*. 2013. p. 1-11. <http://dx.doi.org/10.1017/S0033291713002596>
- Siapas AG, Lubenov EV, Wilson MA. Prefrontal phase locking to hippocampal theta oscillations. *Neuron*. 2005; 46:141–151. <http://dx.doi.org/10.1016/j.neuron.2005.02.028>. [PubMed: 15820700]
- Sirota A, Montgomery S, Fujisawa S, Isomura Y, Zugaro M, Buzsáki G. Entrainment of neocortical neurons and gamma oscillations by the hippocampal theta rhythm. *Neuron*. 2008; 60:683–697. <http://dx.doi.org/10.1016/j.neuron.2008.09.014>. [PubMed: 19038224]
- Steriade M, McCormick DA, Sejnowski TJ. Thalamocortical oscillations in the sleeping and aroused brain. *Science*. 1993; 262:679–685. [PubMed: 8235588]
- Swanson LW. A direct projection from Ammon's horn to prefrontal cortex in the rat. *Brain Res*. 1981; 217:150–154. [PubMed: 7260612]
- Wheeler AL, Teixeira CM, Wang AH, Xiong X, Kovacevic N, Lerch JP, McIntosh AR, Parkinson J, Frankland PW. Identification of a functional connectome for long-term fear memory in mice. *PLoS Comput Biol*. 2013; 9:e1002853. <http://dx.doi.org/10.1371/journal.pcbi.1002853>. [PubMed: 23300432]
- Young CK, McNaughton N. Coupling of theta oscillations between anterior and posterior midline cortex and with the hippocampus in freely behaving rats. *Cereb Cortex*. 2009; 19:24–40. <http://dx.doi.org/10.1093/cercor/bhn055>. [PubMed: 18453538]
- Zeng LL, Shen H, Liu L, Wang L, Li B, Fang P, Zhou Z, Li Y, Hu D. Identifying major depression using whole-brain functional connectivity: a multivariate pattern analysis. *Brain*. 2012; 135:1498–1507. <http://dx.doi.org/10.1093/brain/aws059>. [PubMed: 22418737]

**Fig. 1.**

Experimental design. A) Illustration of a rat brain horizontal section roughly 5.3 mm ventral from bregma (Paxinos and Watson, 1998). Black circles show approximate target locations for the bilateral IL stimulating/recording electrodes and the VH stimulating electrode. B) Nissl-stained coronal sections showing example electrode tracks and estimated tip location in one rat brain for both the IL (left) and hippocampal (right) electrodes. Arrows point to estimated electrode tip locations. C) Timeline of epochs within a session, for all non-injection sessions. D) Timeline of treatment and recording sessions. Recordings were performed on the day before treatment, following 1 and 10 days of treatment, and 1, 10, and 11 days after treatment ended; on Post-Day 1 and 11 rats were treated with either fluoxetine or saline (dashed lines).

**Fig. 2.**

LFP coherence and amplitude across days. A) Coherence spectra for VH and IL LFP recordings for DBS-treated rats (black) and sham-treated animals (gray) during the spontaneous behavior epochs on days 0, 1, 10, and post-10 (top to bottom panels; mean  $\pm$  s.e.m.). Inset in Day 10 panel shows the inverse of the statistical probability ( $1/p$ ) that values from both groups were sampled from the same distribution, dashed horizontal line is the 99% confidence interval. A robust effect of DBS was observed only after 10 days of treatment in the 2–4 Hz range. B) Difference between 2–4 Hz, VH-IL coherence across days of treatment (error bars are s.e.m.). C) LFP spectral density in the IL, relative to the maximum amplitude within the 6 to 10 Hz (theta) band, following 10 days of treatment. No differences were observed in relative signal amplitude between DBS- and sham-treated animals at any frequency bin. D) Amplitude of 2–4 Hz-to-theta LFP signals in the IL across treatment days. E & F) As in C & D respectively, but for VH. In contrast with IL, rats treated with sham stimulation appeared to have stronger 2–4 Hz patterns than DBS-treated rats after 10 days of treatment.

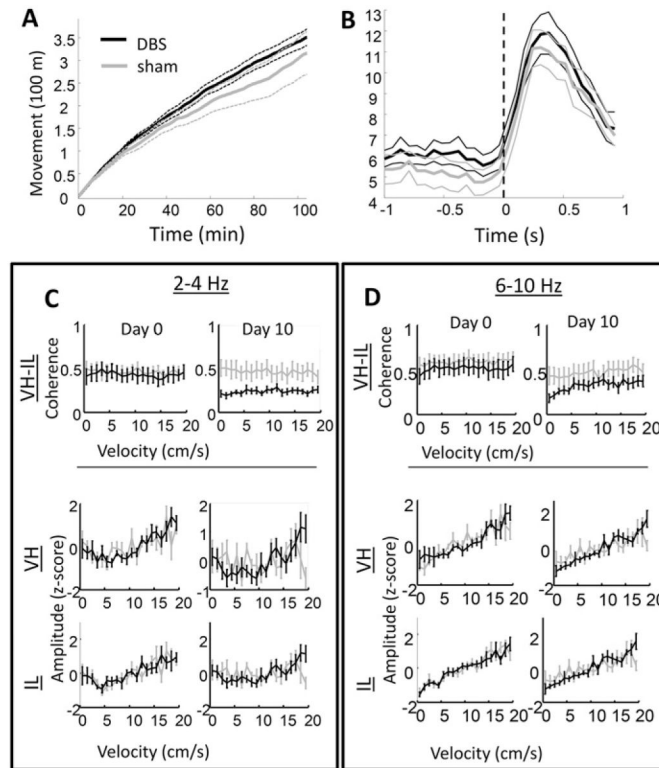


**Fig. 3.**

Movement and coherence. A) Cumulative head movements over the course of 100 min during the Day 10 session for DBS (black) and sham (gray) treated rats. There were no significant differences between groups in the amount the rats moved during the session. B) Head movement responses to the auditory stimulus, also on session Day 10. The orienting, or startle, movements reached a maximum around 300 ms after cue onset, but neither latency nor magnitude of the movements differed between the two treatment groups. C) The 2–4 Hz coherence between VH and IL (top panels) and relative amplitude within each region (middle and bottom panels) on Day 0 (left column) and Day 10 (right column) across velocity bins. In this case, relative amplitude refers to value z-scores across velocity bins; i.e., the middle and lower plots illustrate only whether or not DBS and sham rats differed in the degree to which the strength of 2–4 Hz signals were affected by the rat's movement speed. Although signal amplitude appeared to be affected by speed, coherence between regions did not, and coherence in DBS-treated rats differed from sham controls across all velocity bins (upper right panel). D) As in C, but for theta patterns. Theta amplitude was related to movement speed in both treatment groups.

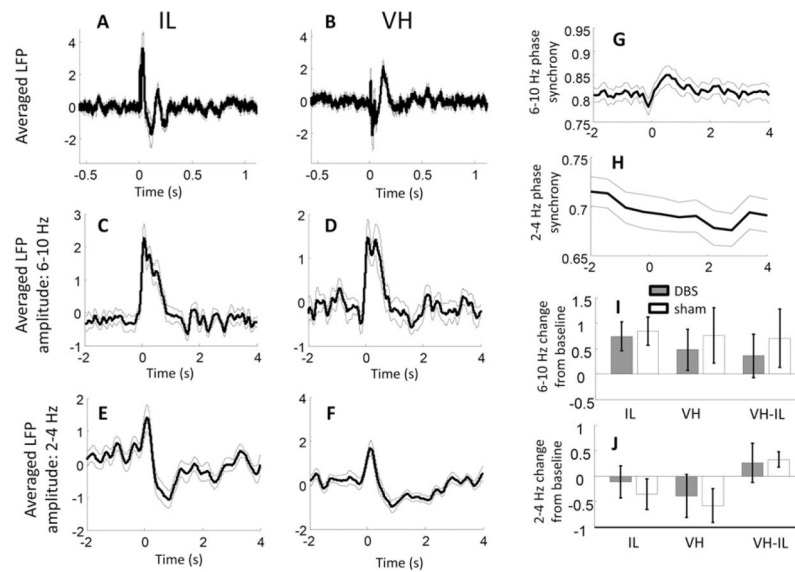


**Fig. 4.**

Neural response to auditory stimulation. A & B) The averaged LFP (i.e., “event related potential,” or ERP) aligned over presentations of the auditory stimulus (zero on x-axis) on recording Day 0, for IL (A) and VH (B) electrodes. Thin lines above and below thicker trace are s.e.m. of values across rats. Several notable components appear in the across-animal averages, although these are difficult to interpret since precise electrode positions differed between animals, resulting in different fields of electrical sources and sinks. C & D) Averaged LFP theta amplitude for IL (C) and VH (D) electrodes on Day 0. LFP signals were filtered and rectified before averages were computed. Theta amplitude increased strongly in both recorded regions for nearly one second following stimulus presentation. E & F) Averaged LFP 2–4 Hz amplitude for IL (E) and VH (F) electrodes on Day 0. In contrast with theta amplitude, 2–4 Hz signals decreased following stimulation. Note that the initial early peak is likely an artifact from an initial broadband activity spike following stimulus onset. G) VH-IL theta phase synchrony, aligned and averaged across presentations of the auditory stimulus. Theta synchrony increased in the seconds following stimulus onset, suggesting that the theta amplitude increases in the two regions (C & D) were in phase with one-another. H) VH-IL 2–4 Hz phase synchrony averaged across presentations of the auditory stimulus. Synchronization decreased in the seconds following stimulus onset on Day 0. I) Degree of change, in standard deviations, of theta amplitude (first and second bar pairs) and coherence (third bar pair) for DBS (filled bars) and sham (unfilled bars) rats on treatment Day 10. There was no evidence for a differential effect of the auditory stimulus in DBS- compared with sham-treated animals. J) Same as in I, but for 2–4 Hz coherence. Once again, no differences were observed between DBS and sham-treated animals in the neural response to auditory stimuli.



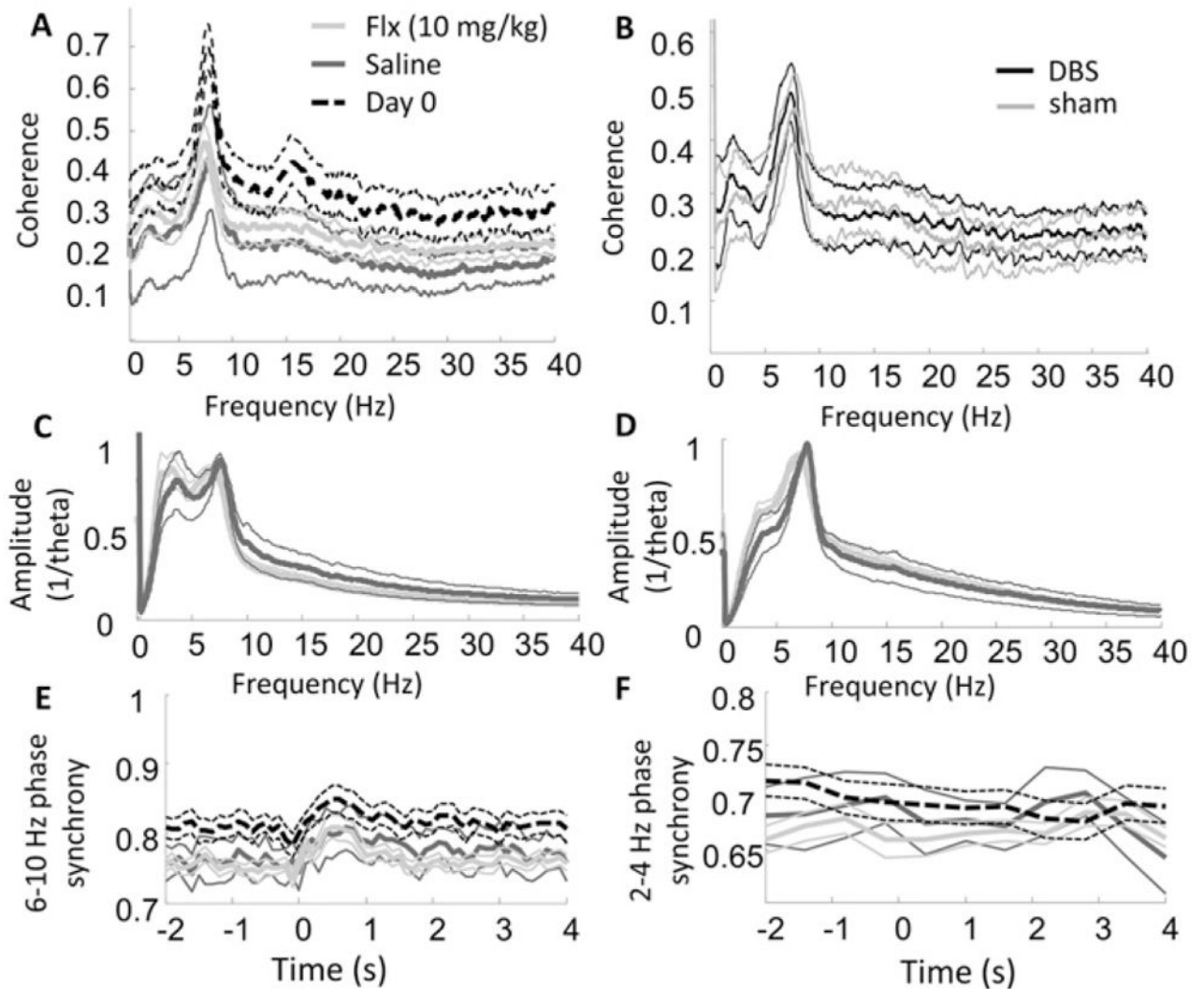


**Fig. 5.**

LFP coherence and amplitude following fluoxetine vs. saline injections. A) VH-IL LFP coherence spectra for fluoxetine (10 mg/kg; light-gray), saline (dark-gray), and on the pre-treatment, Day 0 (dashed black lines). Although coherence was generally reduced following both injections, there were no observable differences between fluoxetine and saline treatments. B) VH-IL LFP coherence spectra for DBS (black) and sham (gray) treatment groups on the day of fluoxetine administration. There were no observable interactions between stimulation and fluoxetine. C & D) Spectral amplitude of LFP patterns relative to theta amplitude in the IL (C) and VH (D). Colors same as in part A. No differences were observed on fluoxetine versus saline days. E & F) Phase synchrony in the theta (E) and 2–4 Hz (F) band, averaged across presentations of the auditory stimulus. Colors same as in part A. No differences were observed in the two treatment groups.